Kufa Journal of Engineering
Vol. 10, No. 4, October 2019, P.P. 53-65
Received 29 March 2019, accepted 2 June 2019

3D CFD SIMULATION AND EXPERIMENTAL STUDY OF A WATER JET IMPINGEMENT

Saeed R. Yassen[1]

[1] Lecturer (PhD), Chemical and Petrochemical Engineering Department, Salahaddin University-Erbil, Erbil, Kurdistan, Iraq. Email: Saeed.yassen@su.edu.krd

HTTP://DX.DOI.ORG/10.30572/2018/KJE/100405

ABSTRACT

To investigate the reaction forces produced by the change in momentum of a water jet, an experimental and computational fluid dynamics (CFD) study are carried out. In the experiment, the water jet forces on a test horizontal hemispherical cup are measured. ANSYS CFX simulation code is used to provide a 3D CFD simulation of a circular cross section water jet released from a nozzle and moves upward in the air before striking a horizontal hemispherical cup and a flat plate. The progress in the CFD simulation within the last decade make it possible to analyze and visualize the flow pattern of complex multiphase free surface fluid flow. The simulated forces of the vertical water jet against a horizontal hemispherical cup using ANSYS CFX code are compared with the experimental forces generated by the water jet as it strikes a hemispherical cup. A good agreement is found in the CFD results compared with the experimental results. 21.649 % was the maximum percent difference recorded at 0.245 kg/sec flowrate and 0.484 % was the minimum percent difference at 0.368 kg/sec flowrate.

KEYWORDS

Water Jet Impingement, Computational Fluid Dynamics.

1. INTRODUCTION

Impact of a jet test-rig enables experiments to be conducted on the impingement force produced on vanes when a water jet strikes a vane. Impingement force can be defined as the rate at which momentum changes in a system (Cengel and Clmbala, 2006). When a water jet is deflected by a solid surface the water momentum changes because the direction changes and it, therefore, exerts a force on that surface. The study of these impingement forces is an essential step in the subject of fluid mechanics that can be applied to hydraulic turbines such as the impulse turbine and Pelton wheel. In these types of water turbines, the kinetic energy of water jet extracts when strikes the blades or buckets on the rim of the runner turbine where the kinetic energy converts into mechanical work (Yassen, 2014). Hydraulic energy is one of the most attractive renewable energy (Obayes and Qasim, 2017; Kapooria, 2009). It is necessary for the researchers understand how the water jet deflection produces a force on the vanes, in order to correctly understand how the impulse turbine (a Pelton wheel, for example) works. They also need to know how this force is influenced by the rate of flow in the jet.

Hereafter the previous studies on the impact of jet are presented, Roshane Nanayakkara uploaded a work for Swinburne University of Technology, school of engineering to investigate the reaction forces produced by the impact of the water jet. Impact of jet rig was used to experimentally investigate the water force on to variety type of target vanes. The results of the experiments indicated that the theoretical calculated force was at all cases lower than the experimentally measured force. The maximum percentage error was below 25 % (Nanayakkara, 2019).

Qusai W. Al-Qudah, 2019 undertook an experimental investigation to investigate the impact of a water jet. The experiment was carried out on an impact of a jet rig at university of Jordan. The main parts of the rig were the nozzle with 1 cm diameter from which the water issues vertically to strike a hemispherical curved or flat plate. A swinging metal level with an air bubble balancer is fitted on it to indicate the swinging metal arm’s horizontal position. A pan for carrying weights. The transparent Plexiglas cylinder for gathering and passing the water through a sink to volume evaluation tank. The pump and control valve used to increase and control the water. According to this investigation the force resulted from the impact of the water jet increases with increasing the flowrate. The experimental measured forces showed larger values than the theoretical calculated ones due to the losses in the experimental rig (Al-Qudah, 2019).

Vrushiket Patil, 2019 presented an experimental investigation to study the relation between the force produced and the change of momentum when a water jet strikes a vane. This experiment resulted in an important conclusion that experimentally force exerted by jet on hemispherical vane was more than that of flat plate and almost double to that of flat plate force (Patil, 2019).

The reaction forces produced by the impact of the water jet were determined by Jain et al. They conducted an experimental investigation to determine the magnitude of the water forces on a hemispherical curved or a flat plate. The experimental apparatus consists of a nozzle, a hemispherical cup or a flat plate, a flow meter, a spring retainer, plumbing for recirculating the water. The results of Jain et al experiments revealed that the error between force values increase with increasing the flowrate (Jain et al, 2017).

The main purpose of the present work to enable the researchers to visualise the fluid flow and analyze the force impingement produced by a jet of water as it impinges on a surface by using ANSYS CFX simulation code.

2. NEXPERIMENT METHOD

2.1. Experimental apparatus

Experiments were conducted on an impact of a jet rig in fluid mechanics' laboratory, mechanical department, college of engineering, salahaddin university-erbil. The impact of the jet rig comprises of a transparent cylinder containing a vertically tapered nozzle and a test hemispherical cup. The cylinder is on legs and mounts on the top of the hydraulic bench. The nozzle, supplied by the hydraulic bench, produces a high-velocity jet of water, which hits the test hemispherical curved plate. The test hemispherical curved plate connects to a weigh beam assembly with an air bubble balancer, which indicates the metal level horizontal position and a pan for carrying weights. A drain tube in the base of the cylinder directs water back into the hydraulic bench, allowing accurate flow rate measurement as shown in Fig. 1.

2.2. Preparing and performing the experiment

To perform experiments, investigators level the apparatus and ensure the balance arm is horizontal, and then they put a certain weight on the balance arm and open the control valve in order to direct the free jet towards the hemispherical curved plate to bring the arm to its horizontal position. After that, they measure the volume of water gathered and duration of the gathering. Increasing the weight on the balance arm and repeating the test for many times to ensure the accuracy.

Fig. 1. Impact of jet test-rig

3. MODELING AND SIMULATION PROCEDURE

3.1. Geometry creation

Catia v5 computer aided design (CAD) program was used to sketch and design a three-dimensional of the impact of jet as shown in Fig. 2. Proper selection of the region of interest and appropriate simplifications plays a key role in the success of the calculation (De Andrade, et al., 2011). Once the region is defined, a computer model of the geometry is created. This was the first step of defining the geometry of the impact of jet. The "Catia" file was saved and then was imported into the ANSYS CFX Workbench geometry module as an input geometry. The geometry module used ANSYS DesignModeler™ software to create and prepare the geometry for simulation. The next step was to create the computational domain regions of fluid flow as shown in Fig. 3.

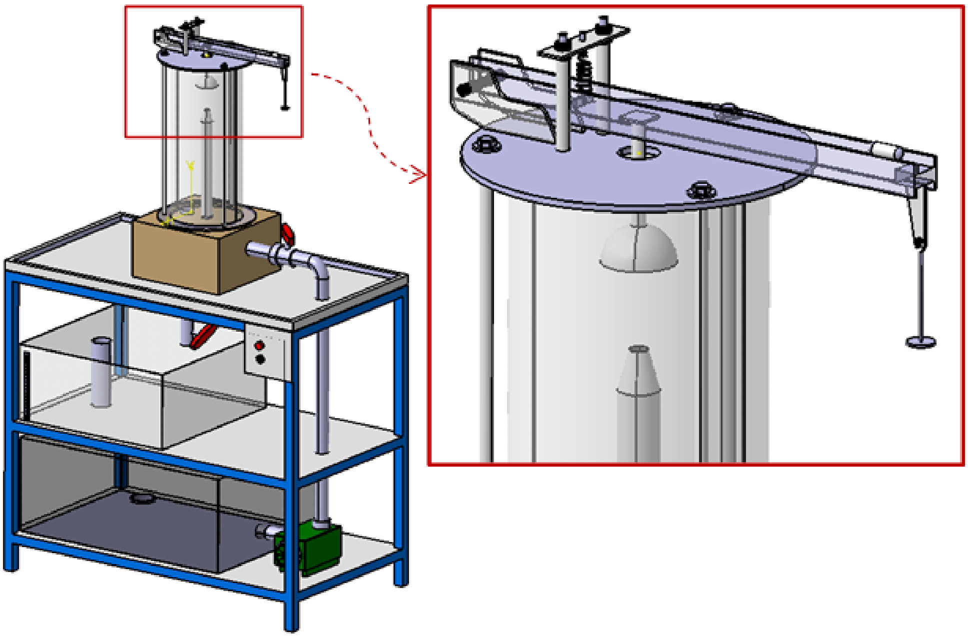

Fig. 2. 3D view of the impact of jet tested.

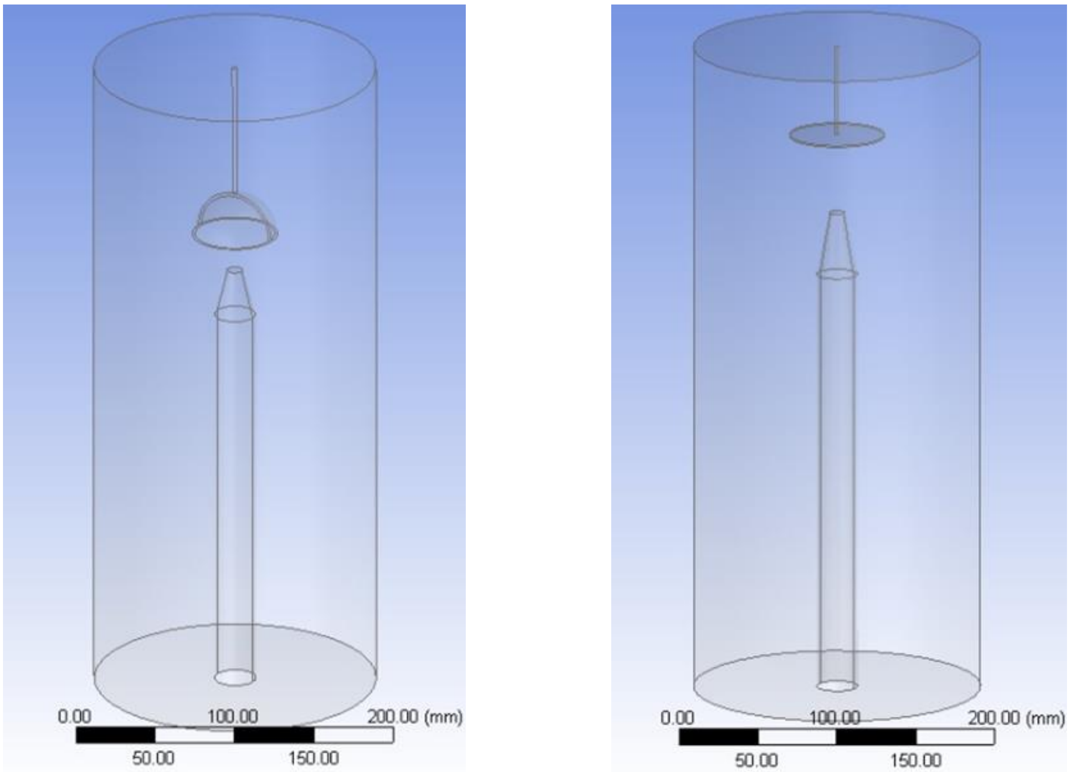

(a) hemispherical cup **(b) Flat plate**

Fig. 3 (a) and (b). Computational domains of the impact of jet tested.

3.2. Grid generation

Ansys CFX meshing tool in workbench was used to grid generation as shown in Fig. 4. A total of 483403 nodes and 1716138 elements were generated. The grid was then imported into the setup module of workbench. The fluid flow simulation parameters were specified. All boundary conditions were explicitly specified. Once the changes in setup module were saved, a new definition file (*.def) was created for later import into CFX solver. That file was the starting point in each simulation.

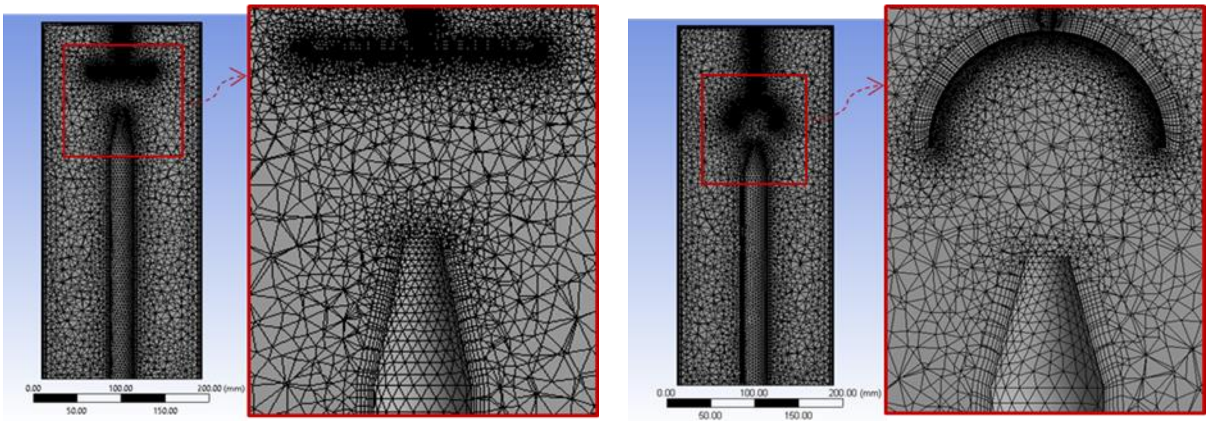

(a) hemispherical cup **(b) Flat plate**

Fig. 4 (a) and (b). Tetrahedral mesh with inflation layers of the half impact of jet tested.

3.3. Geometry creation

The CFX Solver computes the Reynolds-averaged continuity and Navier-Stokes equations with a finite volume and algebraic multigrid method (Simpson and Williams, 2006; Neopane, 2010). The partial differential equations are integrated over the control volumes specified in the region of interest (Gerberkiden, 2007; Nikolic, 2000). It applies the conservation of mass and momentum to the control volumes. These integral equations are translated to algebraic equations by generating approximations for all the terms in the integral equations. The algebraic equations are then solved iteratively. The iterations are due to the non-linear nature of the equations and convergence occurs when the residuals have been reduced by at least four orders of magnitude. This solution process usually required no user intervention and was carried out as a batch process. The simulation results were processed in post-processor.

The Reynolds-averaged continuity and Navier-Stokes equations for incompressible flows are given by the following equations (Hong Gao et al, 2008):

$$\frac{\partial U_i}{\partial x_i} = 0 \qquad (1)$$

$$\frac{\partial}{\partial t}\left(\rho U_i\right) + \frac{\partial}{\partial x_j}\left(\rho U_i U_j\right) = -\frac{\partial p}{\partial x_i} + \frac{\partial}{\partial x_j}\left\{\mu_{eff}\left(\frac{\partial U_i}{\partial x_j} + \frac{\partial U_j}{\partial x_i}\right)\right\} + f_i \qquad (2)$$

where f_i is a component of the body force, ρ the density of the fluid, $\mu_{eff} = \mu + \mu_t$, μ is the molecular dynamic viscosity, μ_t is the turbulent viscosity, U_i, U_j are the mean velocity components and P is the static pressure. For standard $k-\varepsilon$ model, k is the turbulence kinetic energy and ε is the rate of dissipation. The following transport equations are used obtained k and ε:

$$\rho\frac{\partial k}{\partial t} = \frac{\partial}{\partial x_i}\left\{\left(\mu + \frac{\mu_t}{\sigma_k}\right)\frac{\partial k}{\partial x_i}\right\} + G_k - \rho\varepsilon \tag{3}$$

$$\rho\frac{\partial \varepsilon}{\partial t} = \frac{\partial}{\partial x_i}\left\{\left(\mu + \frac{\mu_t}{\sigma_\varepsilon}\right)\frac{\partial \varepsilon}{\partial x_i}\right\} + C_{1\varepsilon}\frac{\varepsilon}{k}G_k - C_{2\varepsilon}\rho\frac{\varepsilon^2}{k} \tag{4}$$

Where G_k represents the generation of the turbulence kinetic energy

$$G_k = -\rho\overline{u_i' u_j'}\frac{\partial U_j}{\partial x_i} \tag{5}$$

$$k = \frac{1}{2}\overline{u_i' u_i'}, \qquad \varepsilon = \nu\frac{\overline{\partial u_i' u_i'}}{\partial x_j \partial x_j} \tag{6}$$

The turbulent (or eddy) viscosity, μ_t, is computed by combining k and ε as follows;

$$\mu_t = \rho C_\mu \frac{k^2}{\varepsilon} \tag{7}$$

In these equation, the empirical constant $C_{1\varepsilon} = 1.44$, $C_{2\varepsilon} = 1.92$ and $C_\mu = 0.09$ (ANSYS, 2017)

4. RESULTS AND DISCUSSION

The results module in the post-processor was used to analyse and visualise the simulation results. Vector plots, like velocity vectors and streamlines, show the direction and magnitude of the fluid flow. It also enabled the visualization of the water volume fractions into the computational domain of the impact of jet, throughout the computational domain. The results of the CFD simulations revealed the complex nature of the internal flow of the water impact of jet and allowed better analysis and understanding to the flow structure. The fluid flow pattern is strongly influenced by the shape of the vane. In Figs. 5(a) and 6(a), the three-dimensional water superficial velocity streamlines and water superficial velocity vectors, were plotted for entire impact of jet. These streamlines and vectors show the complexity of the turbulent two-phase flow from the nozzle sticking the hemispherical cup and flat plat respectively. Figs. 5(b) and 6(c) illustrate the water volume fraction contour at the mid span of the impact of jet. A well-defined interface between the air and water homogenous flow with a free surface flow can be observed. Figs. 5(c), 5(d), 6(a) and 6(b) clearly show the water superficial velocity vectors in the impact of jet. They show that the maximum velocities are at the nozzle outlet.

The water superficial velocity streamline of single-trajectory water flow line was plotted for hemispherical cup and flat plate as shown in Figs. 7 and 8. These figures clearly show the complex three-dimensional water pathline which is directed by the vertical nozzle to strike the hemispherical cup or flat plate. It is important to note that the water superficial velocity details are evidently different to those of Figs. 9 and 10. Changing the obstacle shape from hemispherical cup to flat plate changed the flow structure. Fig. 9 shows the water superficial velocity at hemispherical cup is rather low around the impingement area and over the hemispheric cup compared with the Fig. 10. This can be explained, firstly, by the collision loss increases and friction loss also increases as the hemispherical cup' passage is longer than the flat plate one and curved, secondly once the water hits the center of the hemispheric cup the only way it can travel is downwards and hence come in the way of the water coming from the jet causing dissipate in the energy of water jet.

Comparison of ANSYS CFX simulation results of the three-dimensional full-scale model with the experimental results is shown in Figs. 11 and 12. As can be seen the impingement force of the water jet shows good agreement between simulation and experiment. Figs. 13 and 14 shows the force of the water striking the flat plate changes linearly with the mass water flowrate and the impingement water velocity, respectively.

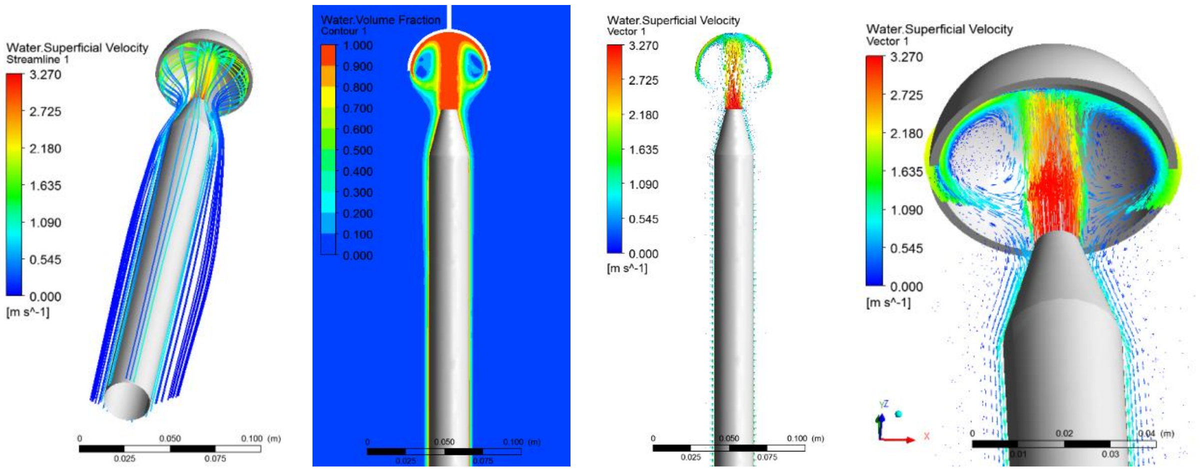

(a) 3D water streamlines for hemispherical cup.

(b) Water volume fraction contours at mid span of hemispherical cup.

(c) Velocity vectors at mid span of hemispherical cup.

(d) Enlargement of velocity vectors at mid span of hemispherical cup.

Fig. 5 (a) to (d). Fluid behaviour inside the hemispherical cup.

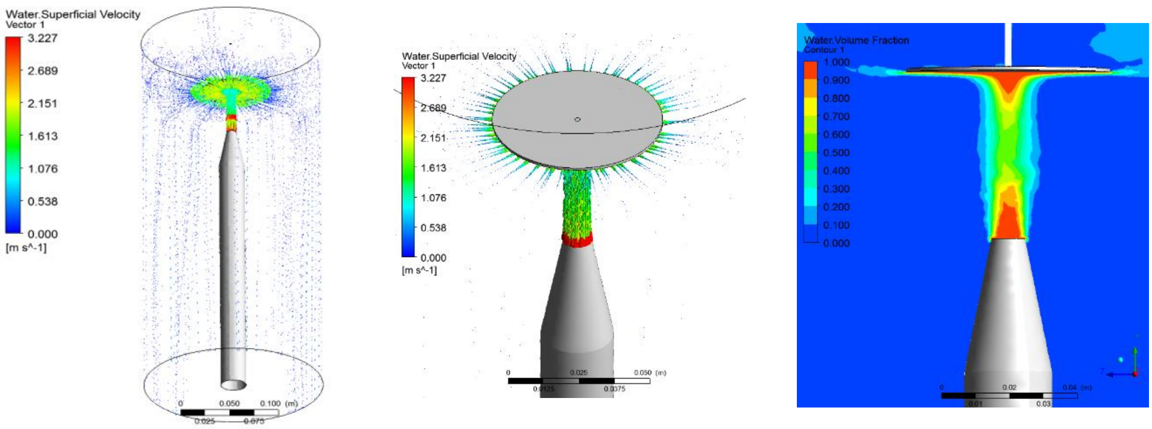

(a) 3D Water velocity for flat plate. **(b) Enlargement of velocity vectors for flat plate.** **(c) Water volume fraction contours at mid span of flat plate.**

Fig. 6 (a) to (c). Fluid behaviour on the flat plate.

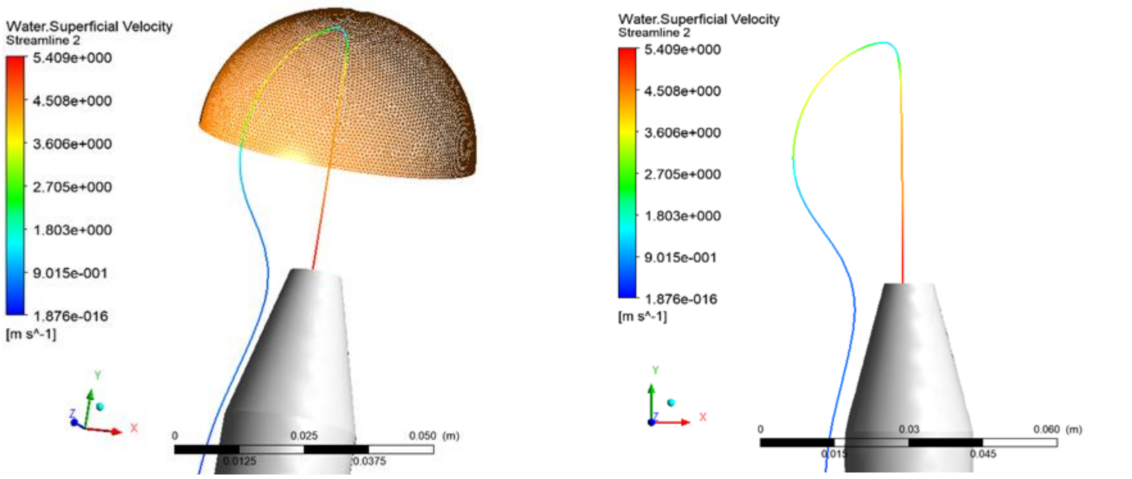

(a) A single-trajectory water flow line for hemispherical cup as viewed with the cup. **(b) A single-trajectory water flow line for hemispherical cup as viewed without the cup.**

Fig. 7 (a) and (b). 3D water pathline for hemispherical cup.

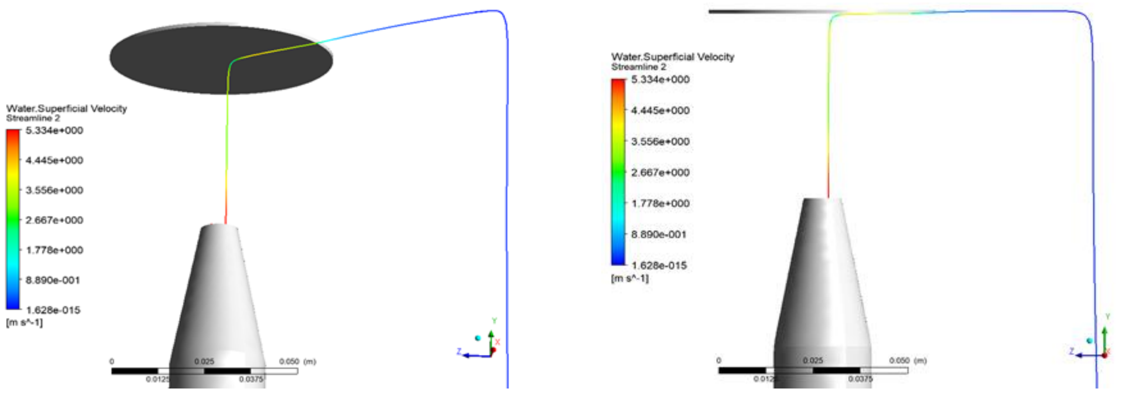

(a) A single-trajectory water flow line for flat plate as viewed with the flat plate. **(b) A single-trajectory water flow line for flat plate as viewed without the flat plate.**

Fig. 8 (a) and (b). 3D water pathline for flat plate.

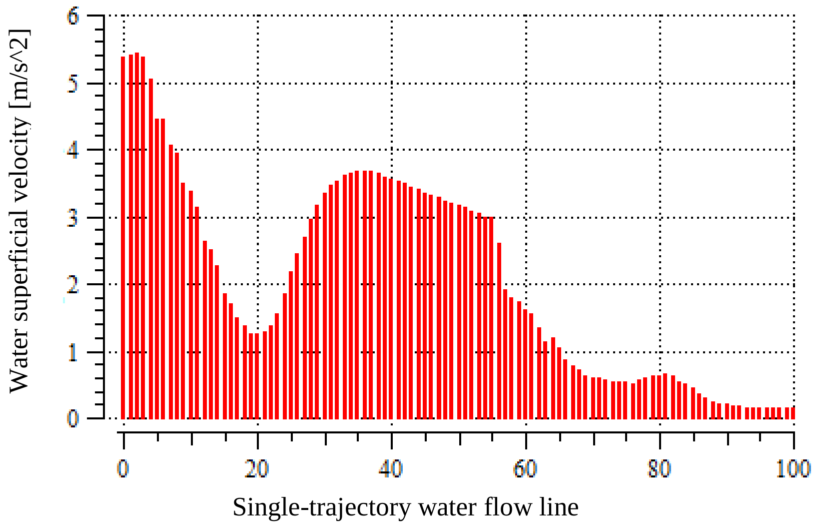

Fig. 9. Water superficial velocity of single-trajectory water flow line for hemispherical cup.

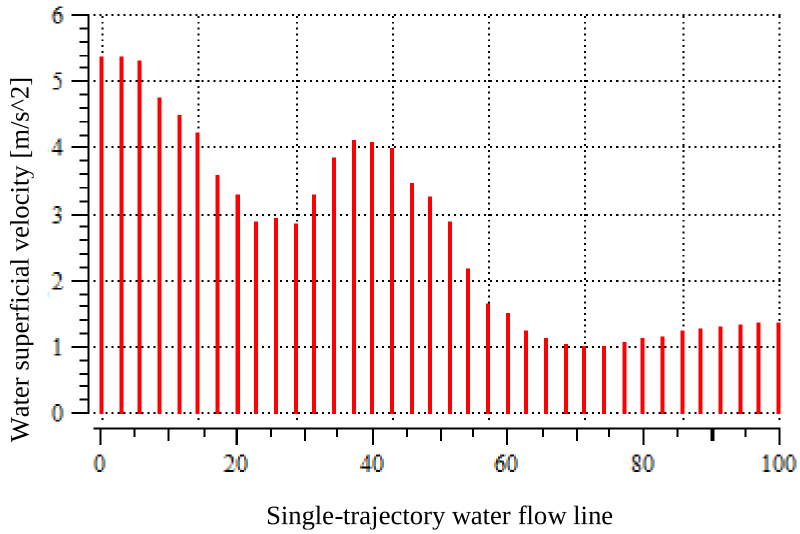

Fig. 10. Water superficial velocity of single-trajectory water flow line for flat plate.

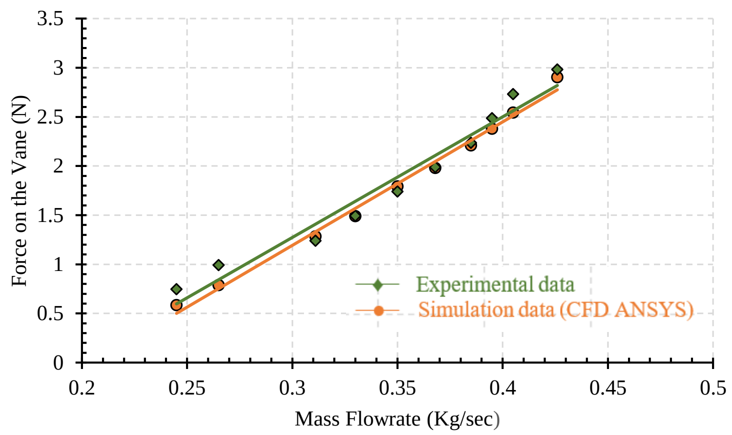

Fig. 11. Comparison of numerical and experimental results of force produced by a water jet striking a hemispherical cup vs mass flowrate.

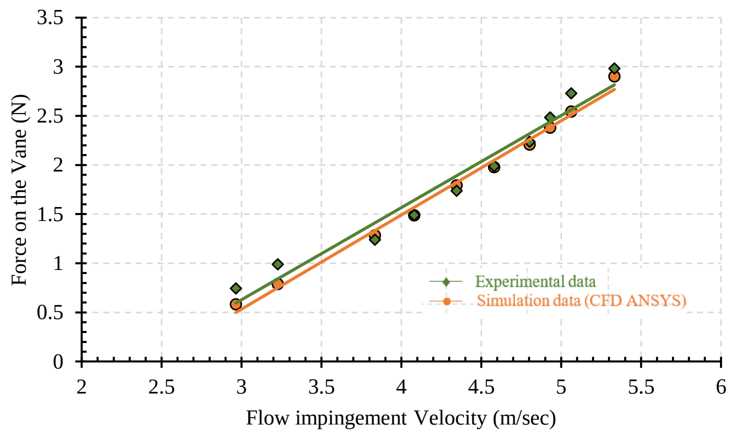

Fig. 12. Comparison of numerical and experimental results of force produced by a water jet striking a hemispherical cup vs flow impingement velocity.

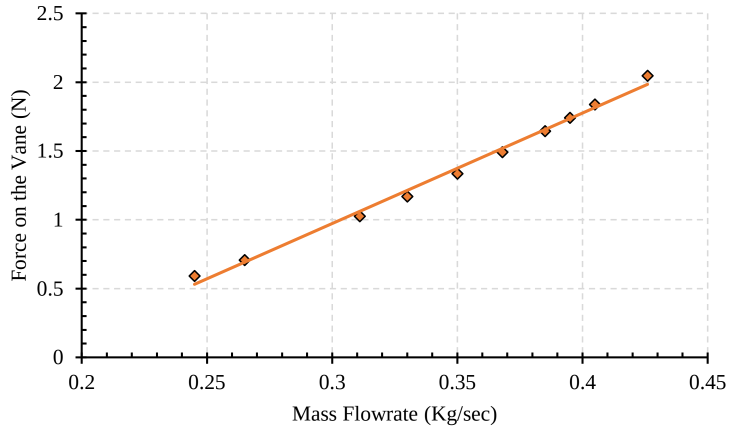

Fig. 13. Numerical results of force produced by a water jet striking a flat plate vs mass flowrate.

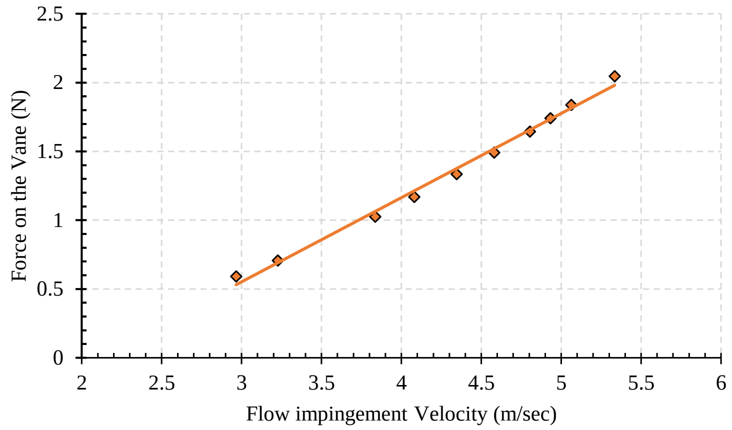

Fig. 14. Numerical results of force produced by a water jet striking a flat plate vs flow impingement velocity.

5. CONCLUSIONS

The pattern of fluid flow and the directions with magnitudes of water jet on a hemispherical cup and flat plate are visualized. The analysis and flow prediction performed by ANSYS CFX simulation code for the influence of shape of the obstacle revealed a fundamental hydrodynamics flow characteristic within the impact of water jet apparatus. With increasing the water jet velocity, the energy extracted from water by the obstacle increase. The force exerted by water jet on hemispherical cup is always more than that of flat plate because of the direction of the water after striking the flat plate is perpendicular to the direction of the water jet released from the nozzle and parallel to the flat plate, therefore, no longer the energy of the water will be extracted by the flat plate.

6. REFERENCES

Al-Qudah, Q. W., accessed: (2019). Impact of Jet, Hydraulic Laboratory [internet], The University of Jordan, Faculty of Engineering and Technology, http://www. icivil-hu.com/Civil-team/Structures%20Section/Structure%20I/Impact%20of%20jet.pdf.

ANSYS, Inc, (2018). "*ANSYS-CFX Solver Theory Guide*", Realease 18.1.

Cengel, Y. A. & Cimbala, J. M., (2006). *Fluid Mechanics: Fundamentals and Applications.* 1st ed. New York: McGraw Hill.

De Andrade, J. et al., (2011). Numerical Investigation of the Internal Flow in a Banki Turbine. *International Journal of Rotating Machinery*, Volume 2011.

Gerberkiden, B. M., (2007). *Effect of Inlet Boundary Conditions on Spiral Casing Simulation*, s.l.: Lulea University of Technology, Master's thesis.

Hong Gao, Wanlai Lin & Zhaohui Du, (2008). Numerical flow and performance analysis of a water-jet axial flow pump. *Ocean Engineering, 35(16), pp. 1694-1614.*

Jain, A. K., Kudal, A. S. & Gupta, V., (2017). TO Verify the momentum Equation by Impact of Jet Apparatus on Flat Plate. *International Journal of Innovative and Emerging Research in Engineering, 4(4).*

Kapooria, R. K., (2009). An Efficiency Assessment Analysis of a Modified Gravitational Pelton-Wheel Turbine. *Journal of Energy in Southern Africa*, 20(4).

Nanayakkara, R., accessed, (2019). Impact of Jet, s.l.: Scribd [internet] available from: https://www.scribd.com/doc/38008443/Impact-of-Jet.

Neopane, H. P., (2010). *Sediment erosion in hydro turbine*, s.l.: Norwegian University of Science and Technology, Doctor's thesis.

Nikolic, Z., (2000). *Three-Dimensional Analysis of a Reactor for the Production of Vimaterals Using CFD Commercial Code Fluent,* s.l.: Oklahoma State University, Master's thesis.

Obayes, S. A. S. & Qasim, M. A. K., (2017). Effect of flow parameters on pelton turbine performance by using different nozzles. *International Journal of Modeling and Optimization,* 7(3).

Patil, V., accessed: (2019). Impact of Jet on Vanes, s.l.: Scribd [internet], available from: https://www.scribd.com/doc/71242319/Impact-of-Jet-on-Vanes.

Simpson, R. G. & Williams, A. A., (2006). *Application of computational fluid dynamics to the design of pico prepeller turbine.* Washington, D.C.: University of the District of Columbia., Proceedings of the International Conference on Renewable Energy for Developing Countries.

Yassen, S. R., (2014). *Optimization of the performace of mirco hyro-turbines generation,* s.l.: University of Hertfordshire, UK, Doctor's thesis.